International Journal of Innovative
Computing, Information and Control
Volume **15**, Number **3**, June **2019**

 ISSN 1349-4198
pp. **1093–1114**

STUDY ON PID CONTROL OF VEHICLE SEMI-ACTIVE SUSPENSION BASED ON GENETIC ALGORITHM

Guoqiang Chen, Shaobin Lv and Jun Dai

School of Mechanical and Power Engineering
Henan Polytechnic University
No. 2001, Century Avenue, Jiaozuo 454003, P. R. China
{ jz97cgq; lyu27bsh }@sina.com; 253175447@qq.com

Received September 2018; revised January 2019

Abstract. *Aiming at the significant differences and the complex mechanical characteristic of the vehicle semi-active suspension between different control methods, a comprehensive study and comparison are conducted between the different proportional-integral-derivative controllers under different road conditions in the semi-active suspension. The semi-active suspension model and the control strategy based on the genetic algorithm are established and proposed for the classical proportional-integral-derivative, the integral separation proportional-integral-derivative and the incomplete derivative proportional-integral-derivative controllers. The optimal parameters of the controllers are obtained by the genetic algorithm. The analysis results show that the performance of the three controllers for semi-active suspension is greatly improved compared with the passive suspension. The dynamic performance of the classical proportional-integral-derivative controller suspension is better than the other two proportional-integral-derivative controllers when the vehicle runs on the same road under different speeds. When the vehicle runs on different roads under the same speed, the adaptive performance of the semi-active suspension controlled by the integral separation proportional-integral-derivative controller is best. The actual road is usually more complicated; therefore, the requirement on the suspension performance of the vehicle is the highest. All in all, the integral separation proportional-integral-derivative controller has the best performance.*
Keywords: Semi-active suspension, Genetic algorithm, Proportional-integral-derivative controller, Suspension performance

1. **Introduction.** The ride comfort and the vehicle handling stability have become the important parameters in the vehicle evaluation standard [1]. The suspension system that connects the wheel and the bodywork plays an important role in the ride comfort and the vehicle handling stability of the vehicle [2]. The suspension is divided into the passive suspension, the semi-active suspension and the active suspension [3,4]. The performance of the passive suspension is barely satisfactory and cannot meet the requirements because its performance cannot be adjusted with the condition of the complicated road surface excitation [5]. The active suspension is rarely used in the expensive vehicle because of its disadvantages of high price, high technical requirements and poor reliability. However, the semi-active suspension has attracted extensive interest because of good smoothness and controllability, high reliability, low cost and adjustable performance [6].

Plenty of research has been done on the semi-active suspension control parameter and method. For example, W. Yang designed and verified the controller for the semi-active suspension by adjusting the damping coefficient [7]. D. Ozgur et al. controlled the active suspension by adjusting the stiffness [8]. Wang et al. added another adjustable damper to

DOI: 10.24507/ijicic.15.03.1093

control the active suspension [9]. An additional control force is added to the suspension by most researchers [10,11], which has been verified to have wide application prospects.

In order to achieve excellent performance, a large number of typical control strategies have been utilized and improved in the semi-active suspension, such as the proportional-integral-derivative (PID) controller, the fuzzy controller and the sliding mode controller. A. B. Kunya and A. A. Ata studied the suspension performance using the fractional-order calculus PID controller [12], and J. X. Tang et al. studied the PID controller in the semi-active suspension [13]. The good control effect of the PID controller has been verified, and the results in [14-17] showed that the bodywork vertical vibration acceleration had been further reduced and improved in the human sensitive frequency range on the aspect of the vehicle ride comfort. The fuzzy controller has also been used in the semi-active suspension control. N. Desai et al. used a fuzzy controller to control the suspension and the results showed that the vehicle ride comfort was greatly improved and the pitch and roll motion was effectively suppressed [18,19]. The fuzzy control suspension has been tested based on the 1/4-car model, the 1/2-car model and the full car, and the control effect was satisfactory with the vehicle acceleration amplitude, the suspension dynamic travel and the tire dynamic displacement significantly reduced [20-22]. Therefore, the smoothness and ride comfort of the vehicle has been improved [23]. The fuzzy PID controller that combines the fuzzy control and the PID control has also been used and the suspension performance is significantly improved [24]. The LQG (linear-quadratic-Gaussian) control, the sliding mode control and the neural network control have been verified efficient in the semi-active suspension. R. Kashani and S. Kiriczi studied the LQG control in the semi-active suspension, and tested the performance under the coordinated control of the vehicle ride comfort and handling stability with the steering wheel single-cycle sinusoidal input and step input on the A-grade and C-grade roads respectively [25]. Y. Jin et al. studied the endocrine LQR control and the simulation results showed that the endocrine LQR control was of good quality and had good adaptability in changing operation parameters, and the suspension damping effect was better than the traditional LQR control [26]. The research results showed that the sliding mode controller had stable performance and improved the performance parameters of the suspension system [27,28]. H. Li et al. used neural network method to control the suspension, and the simulation results showed that the robust neural network control had the small tracking error and the ability of self-adaptive adjustment, and could reduce the vertical vehicle vibration amplitude and improve the ride comfort [29,30]. B. K. Song et al. studied the fuzzy sliding mode control and the results showed that the proposed controller can provide better control ability of vibration control with lower consumed power compared with two existing fuzzy sliding mode controllers [31]. H. Souilem and N. Derbel used adaptative neuro-fuzzy controller to control the suspension system, and simulation results showed that this control exhibited an improved ride comfort and good road holding ability and indicated that the proposed control system has superior performance at adapting random road disturbance for vehicle's suspension [32].

Because of the saturated limiting and the nonlinear constraint in the controller and the semi-active suspension, the system is extremely complicated. Therefore, it is very hard to obtain the optimum parameter through theoretical derivation in the controller. Accordingly, the optimization algorithm has been used to improve the control performance. J. Meng et al. used the genetic algorithm to optimize the PID controller in the semi-active suspension [33]. W. Wang et al. used the cultural algorithm to optimize the fuzzy PID controller [34]. The particle swarm algorithm has also been widely used to optimize the controller in the active and semi-active suspension [35-37]. On the whole, the optimization can significantly improve the control performance.

Quite a number of novel and improved control methods for the semi-active suspension have been proposed and tested by a large number of scholars. The control method generally comes from the typical control method, such as PID controller, the fuzzy controller, the LQR controller and the sliding mode controller. The PID controller has the advantages of simple structure, fast control response and good control performance. Based on the PID controller, a variety of different control methods have been produced, for example, the fuzzy PID controller and the neural network PID controller. The PID controller can be subdivided into the classical PID controller, the integral separation PID controller, the incomplete differential PID controller, and so on. The PID controller can be simply designed for second-order plants. However, the design of PID controller suitable for third-order plants is quite difficult. Through the improvement of the PID controller, the PID control has a wider application range. For example, P. Pannil et al. proposed a proportional-integral-derivative-acceleration (PIDA) controller using the Kitti's method for third-order plants [38]. Simulation results confirm that the proposed PIDA controller provides the satisfied performances. Every PID controller has its unique parameters and exhibits significant differences in application. A comprehensive study and comparison between the different PID controllers in the semi-active suspension are clearly of great benefit.

To study the performance characteristics of the semi-active suspension controlled by the different PID controllers, the performance of the semi-active suspension is analyzed. The performance changes and correlations of the semi-active suspensions controlled by the different PID controllers are obtained through the analysis of bodywork acceleration, speed, displacement and suspension deflection. To analyze the adaptive performance of the semi-active suspensions controlled by the different PID controllers, the performance of the semi-active suspension is analyzed on different roads and at different speeds. The results show that the PID controller can effectively improve the performance of the semi-active suspension. The performance characteristic of the semi-active suspension is obtained when the vehicle runs on different roads at different speeds. The research result lays a solid foundation for the related experiments, dynamic analysis and structural optimization of the semi-active suspension. Therefore, the paper proposes to analyze and compare the performance of the semi-active suspension using the above PID controllers on different roads and at different speeds.

The paper is organized as follows. In Section 2, the semi-active suspension mathematical model and road model are established, and the solving method is proposed. The control and optimization method is proposed and given based on the classical PID controller, the integral separation PID controller, the incomplete differential PID controller in Section 3. The results under different vehicle speeds and different road surfaces conditions are given and discussed in Section 4. Finally, the paper is summarized in Section 5.

2. **Mathematical Model.**

2.1. **Semi-active suspension model.**

As shown in Figure 1, the semi-active suspension model of a 1/4 vehicle can be simplified into four parts. The bodywork, the power system and the bodywork accessories are called the spring-loaded part. The elastic element, the damper and the control resistance device are called the suspension. The wheel hub, the brake actuator, the wheel, etc., are called the unsprung part. The tire is simplified as a resilient element.

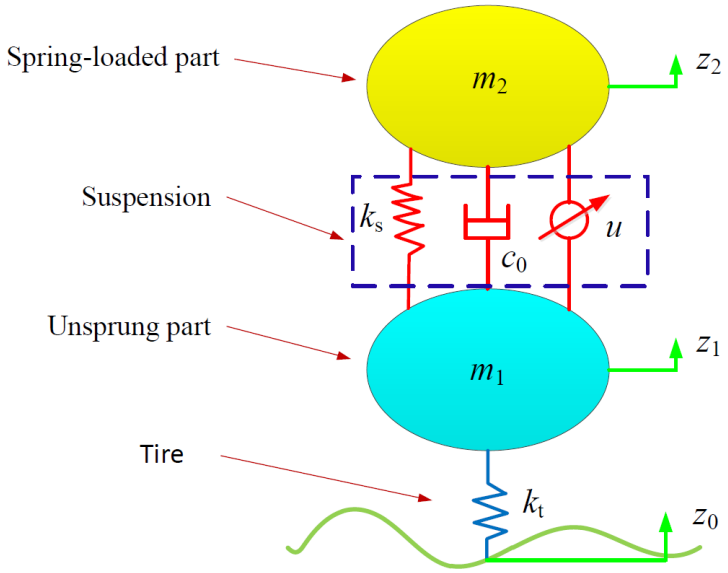

FIGURE 1. Semi-active suspension model

According to Newton's second law, the mathematical model of the semi-active suspension system can be expressed as

$$\begin{cases} m_2\ddot{z}_2 + c_0(\dot{z}_2 - \dot{z}_1) + k_s(z_2 - z_1) + u = 0 \\ m_1\ddot{z}_1 + c_0(\dot{z}_1 - \dot{z}_2) + k_s(z_1 - z_2) + k_t(z_1 - z_0) - u = 0 \end{cases} \tag{1}$$

where m_1 and m_2 are the masses of the unsprung part and the spring-loaded part respectively; k_s and k_t are the stiffness coefficient of the semi-active suspension and the tire respectively; c_0 is the damping coefficient of the damper; z_1, z_2 and z_0 are the displacement of the unsprung part, the spring-loaded part and the road excitation respectively; and u is the controlling force.

In order to solve the differential equation by the Runge-Kutta method, Equation (1) is converted into four first-order differential equations. If $z_3 = \dot{z}_1$, $z_4 = \dot{z}_2$, Equation (1) can be expressed as

$$\begin{cases} \dot{z}_1 = z_3 & \text{(a)} \\ \dot{z}_2 = z_4 & \text{(b)} \\ \dot{z}_3 = \dfrac{c_0(z_4 - z_3) + k_s(z_2 - z_1) + k_t(z_0 - z_1) + u}{m_1} & \text{(c)} \\ \dot{z}_4 = \dfrac{c_0(z_3 - z_4) + k_s(z_1 - z_2) - u}{m_2} & \text{(d)} \end{cases} \tag{2}$$

Equation (2) is constructed by four first-order differential equations. The suspension displacement value is obtained by Equation (2a). The bodywork displacement value is obtained by the first-order differential Equation (2b). The suspension speed value is obtained by the first-order differential Equation (2c). The bodywork speed value is obtained by the first-order differential Equation (2d).

Equation (2) can be represented by a matrix, which can be expressed as

$$\dot{\mathbf{Z}} = \mathbf{f}(\mathbf{Z}, t) \tag{3}$$

where $\mathbf{Z}$ and $\mathbf{f}$ can be expressed as

$$\mathbf{Z} = [z_1, z_2, z_3, z_4]^{\mathrm{T}} \tag{4}$$

$$\mathbf{f} = \begin{bmatrix} 0 & 0 & 1 & 0 \\ 0 & 0 & 0 & 1 \\ -\dfrac{k_\mathrm{s}+k_\mathrm{t}}{m_1} & \dfrac{k_\mathrm{s}}{m_1} & -\dfrac{c_0}{m_1} & \dfrac{c_0}{m_1} \\ \dfrac{k_\mathrm{s}}{m_2} & -\dfrac{k_\mathrm{s}}{m_2} & \dfrac{c_0}{m_2} & -\dfrac{c_0}{m_2} \end{bmatrix} \mathbf{Z} + \begin{bmatrix} 0 \\ 0 \\ \dfrac{k_\mathrm{t}z_0+u}{m_1} \\ -\dfrac{u}{m_2} \end{bmatrix} \tag{5}$$

2.2. **Road model.** The smoothness of the vehicle can be evaluated thorough the road roughness power spectrum and the frequency response of the vehicle system. The road roughness is mainly described by the road power density. The power spectral density of the road can be expressed as [39]

$$G_\mathrm{q}(n) = G_\mathrm{q}(n_0)\left(\frac{n}{n_0}\right)^{-W} \tag{6}$$

where n is the spatial frequency that which contains several wavelengths in a unit length; n_0 is the reference space frequency, $0.1\mathrm{m}^{-1}$; $G_\mathrm{q}(n_0)$ is the roughness coefficient of the road; W is the frequency index that determines the frequency structure of the pavement power spectral density.

The speed power spectral density can be expressed as

$$G_{\dot{\mathrm{q}}}(n) = (2\pi n)^2 G_\mathrm{q}(n) \tag{7}$$

The relationship between the spatial frequency power spectral density and the time-frequency power spectral density of the rode can be expressed as

$$G_\mathrm{q}(f) = \frac{G_\mathrm{q}(n)}{v} \tag{8}$$

where v is the speed of the vehicle, and f is the time frequency and represents the number of waves contained in a time unit.

If the frequency index is 2, the road-time power spectral density can be obtained by Equations (6) and (8), and can be expressed as

$$G_\mathrm{q}(f) = \frac{1}{v}G_\mathrm{q}(n_0)\left(\frac{n}{n_0}\right)^{-2} = G_\mathrm{q}(n_0)n_0^2\frac{v}{f^2} \tag{9}$$

The power spectral density of the road surface speed can be obtained by Equations (6) and (7). It can be expressed as

$$G_{\dot{\mathrm{q}}}(n) = (2\pi n_0)^2 G_\mathrm{q}(n_0) \tag{10}$$

The relationship between the speed and the displacement power spectral density can be expressed as

$$G_{\dot{\mathrm{q}}}(f) = (2\pi f)^2 G_\mathrm{q}(f) = 4\pi^2 G_\mathrm{q}(n_0)n_0^2 v \tag{11}$$

It can be seen from Equation (11) that the power spectral density amplitude of the road speed is only related to the roughness coefficient. For the continuous random road input model, the vehicle speed is also taken into consideration and the white noise speed spectrum is used to describe the road model in time domain. So the random road input function can be expressed as

$$x(t) = 2\pi n_0\sqrt{G_\mathrm{q}(n_0)v}\int_0^t w(t)\mathrm{d}t \tag{12}$$

where $x(t)$ is the vertical displacement excitation of the road surface, and $w(t)$ is the white noise.

3. **Suspension Control Strategy.** The control schematic diagram is shown in Figure 2. The input to the PID controller is the difference between the fixed input signal and the spring-loaded part acceleration. The performance of the suspension is improved by controlling the force using the PID controller.

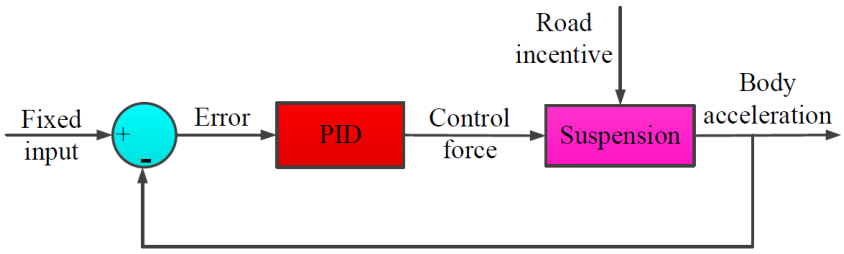

FIGURE 2. Suspension is controlled by PID flow chart.

3.1. **Three different PID controllers.** The classical PID control law can be expressed as

$$u(t) = k_{\mathrm{p}} \times e(t) + k_{\mathrm{i}} \times \int_0^t e(t)\mathrm{d}t + k_{\mathrm{d}} \times \frac{\mathrm{d}e(t)}{\mathrm{d}t} \tag{13}$$

where k_{p}, k_{i} and k_{d} are the coefficients of the proportional, the integral, and the derivative, respectively; and $e(t)$ is the error that changes over the time.

The role of the proportional term is to improve the response speed and adjustment accuracy. When the proportional coefficient in the control system is large, the system has a fast response speed. However, when the proportional coefficient in the control system is large, it is easy for the system to produce overshoot. When the proportional coefficient in the control system is small, the response speed of the system is slow. When the proportional coefficient in the control system is small, the adjustment time is prolonged and the accuracy of system adjustment is reduced. Therefore, the static and dynamic characteristics of the system are poor.

The role of the integral term is to eliminate the system steady-state error and improve the accuracy of the system control. If the integral coefficient is too small, the static difference cannot be eliminated in time, and the function of the integral part can be realized, which directly affects the adjustment accuracy of the system. If the selected coefficient is too large, the system produces an overshoot phenomenon, and even produces an integral saturation phenomenon in the early stage of the response process. The integral separation PID controller can well solve the problem of large overshoot generated by the system. The integral separation PID controller has a threshold. If the error exceeds the threshold, the integral part is eliminated. This will not only avoid excessive overshoot, but also improve the system response speed. If the error is less than the threshold, the integral part is used. This will not only eliminate static differences, but also improve the system accuracy. The integral separation PID controller can be expressed as

$$u(k) = k_{\mathrm{p}}e(k) + k_{\mathrm{i}}\beta \sum_{i=0}^{k} e(i)T + k_{\mathrm{d}}\frac{[e(k) - e(k-1)]}{T} \tag{14}$$

where β is the switching factor. If $e(k) \leq \varepsilon$, the switching factor is 1; if $e(k) > \varepsilon$, the switching factor is 0. And ε is the threshold.

The derivative term can effectively improve the dynamic performance of the system, but it is also easy to introduce high frequency interference accordingly. This problem can be solved by adding a low-pass filter in the PID control system. The low-pass filter is directly added to the PID differential, and it becomes an incomplete differential PID.

The transfer function of the differential term in the incomplete differential PID controller can be expressed as

$$u_{\mathrm{D}}(s) = \frac{k_{\mathrm{p}} T_{\mathrm{D}} s}{T_{\mathrm{f}} s + 1} E(s) \tag{15}$$

The differential equation of differential term in the incomplete differential PID controller can be expressed as

$$u_{\mathrm{D}}(k) + T_{\mathrm{f}} \frac{\mathrm{d}u_{\mathrm{D}}(t)}{\mathrm{d}t} = k_{\mathrm{p}} T_{\mathrm{D}} \frac{e(k) - e(k-1)}{T_{\mathrm{s}}} \tag{16}$$

where T_{f} is the filter coefficient, T_{D} is a differential time constant, and T_{s} is the sampling time.

Equation (16) can also be expressed as

$$u_{\mathrm{D}}(k) = \frac{T_{\mathrm{f}}}{T_{\mathrm{s}} + T_{\mathrm{f}}} u_{\mathrm{D}}(k-1) + k_{\mathrm{p}} \frac{T_{\mathrm{D}}}{T_{\mathrm{s}} + T_{\mathrm{f}}} (e(k) - e(k-1)) \tag{17}$$

If $\alpha = \frac{T_{\mathrm{D}}}{T_{\mathrm{s}} + T_{\mathrm{f}}}$, then $\frac{T_{\mathrm{s}}}{T_{\mathrm{s}} + T_{\mathrm{f}}} = 1 - \alpha$. If $k_{\mathrm{D}} = \frac{k_{\mathrm{p}} T_{\mathrm{D}}}{T_{\mathrm{s}}}$, the differential term of the incomplete differential PID controller can be expressed as

$$u_{\mathrm{D}}(k) = k_{\mathrm{D}}(1 - \alpha)(e(k) - e(k-1)) + \alpha u_{\mathrm{D}}(k-1) \tag{18}$$

So the incomplete differential PID controller can be represented as

$$u(k) = k_{\mathrm{p}} e(k) + k_{\mathrm{i}} \sum_{i=0}^{k} e(i) T + k_{\mathrm{d}} (1 - \alpha) \frac{(e(k) - e(k-1))}{T} + \alpha u_{\mathrm{D}}(k-1) \tag{19}$$

3.2. **Genetic algorithm.** The genetic algorithm is a computational model that simulates the evolutionary process of the biology and genetics. According to the fitness value of the semi-active suspension, the individuals generated by selection, crossover and mutation are screened. If the individual fitness of the semi-active suspension is high, the individual is retained. If the individual fitness of the semi-active suspension is low, the individual is removed. The new population produced is compared with the previous generation. The new population continues to cycle through the above process. When a predetermined condition is satisfied, the optimal individual is obtained.

The basic operations of the genetic algorithm include selection, crossover and mutation. Selection is the process of selecting good individuals in a population to produce new populations. The good individual of the semi-active suspension is more likely to produce the next generation. Crossover is a reproduction phenomenon that simulates the process of biological evolution. Two fine individuals are provided with half of the genes to produce new good individuals. Mutation is the phenomenon of gene mutation under accidental conditions.

The objective function and adaptive value function of the genetic algorithm for the semi-active suspension controlled can be expressed as

$$z = \sqrt{\frac{1}{N} \sum_{t=1}^{N} |\ddot{z}_2|^2} \tag{20}$$

where N is the number of the proper sampling points.

As shown in Figure 3, the optimal control parameters are obtained by using the genetic algorithm. The schematic diagram can be expressed as follows.

Step 1: The initial parameter range is determined. The PID parameter adjustment methods include empirical method, attenuation curve method, critical proportional method and response curve method. The empirical method is also called the trial and

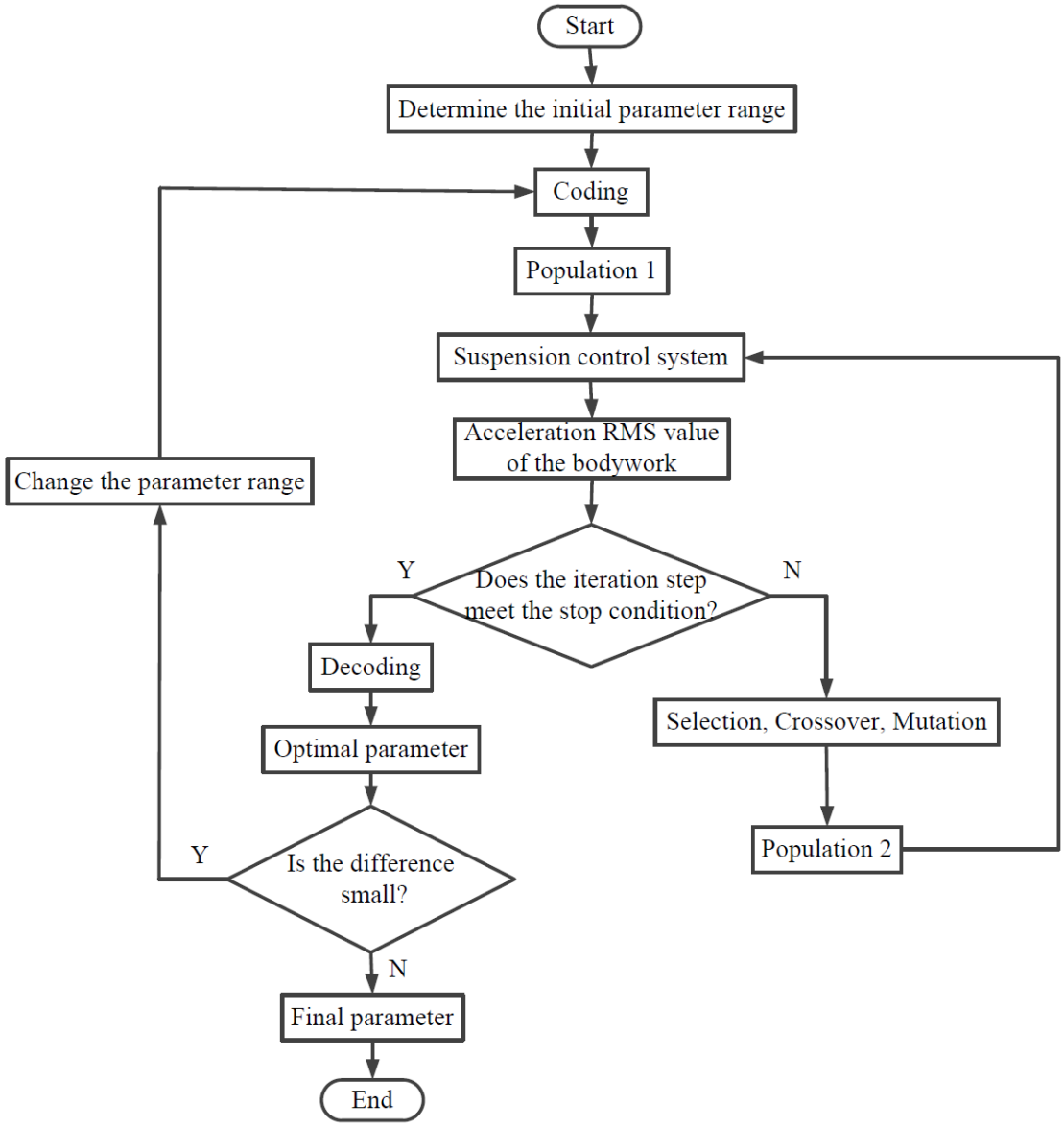

FIGURE 3. Genetic algorithm flow chart

error method. The initial parameter range is obtained based on the good basic parameters of the PID controller. The good basic parameters of the PID controller are obtained through trial and error.

Step 2: According to the calculated accuracy requirements, the parameter range of the variable is coded. Each parameter is represented by a binary string. The string is an object that can be controlled by the genetic algorithm.

Step 3: An initial population 1 is generated randomly. The initial population is randomly selected within the initial parameters range.

Step 4: The generated population corresponding parameters are substituted into the semi-active suspension control system. The bodywork acceleration is obtained through the response characteristics of the semi-active suspension system.

Step 5: The root mean square (RMS) value of the bodywork acceleration is obtained by Equation (20). Because the objective function value and fitness value of the genetic algorithm of this study are the RMS value of the bodywork acceleration, the objective function value and the fitness value of the genetic algorithm are obtained.

Step 6: When the number of iteration steps is less than the predetermined value, the population 1 is operated by selection, crossover and mutation algorithm to generate population 2. Population 2 is better than population 1. Go to Step 4 and repeat the above steps. When the number of iterative steps is equal to the predetermined value, the optimization parameters are obtained by decoding. The optimization parameters are the basic parameters of the PID controller.

Step 7: The optimization result parameter is compared with the parameter range critical value. If the difference between the optimization result parameter and the critical value of the parameter range is small, the parameter range is modified. Go to Step 2 and continue the calculation. If the difference between the optimization result parameter and the critical value of the parameter range is large, the final merit parameter is output.

3.3. **Suspension performance evaluation standard.** According to the relevant regulation, the suspension performance is evaluated by the weighted acceleration RMS value. The vehicle comfort is evaluated by considering the vibration of the seat support surface, the seat back support surface and the foot support surface. The foot comfort is directly determined by the suspension. Therefore, this study only analyzed the vibration of the foot support surface in the vertical direction. The reason is that the human body is more sensitive to the specific range vibration frequencies. And the vibration input at different points and different axial directions have different effects on human comfort level. Regarding the human body's evaluation method for the whole-body vibration, the international standards have made corresponding regulations. According to the international standard ISO 2631, the human exposure to whole-body vibration is evaluated only for frequencies from 0.5 Hz to 80 Hz.

The RMS value of the weighted acceleration can be expressed as

$$a_{\mathrm{w}} = \left[\int_{0.5}^{80} W^2(f) G_{\mathrm{a}}(f) \mathrm{d}f\right]^{\frac{1}{2}} \tag{21}$$

The frequency weighted coefficient of the foot supporting surface in the vertical direction can be expressed as

$$W(f) = \begin{cases} 0.5 & (0.5 < f \leq 2) \\ f/4 & (2 < f \leq 4) \\ 1 & (4 < f \leq 12.5) \\ 12.5/f & (12.5 < f < 80) \end{cases} \tag{22}$$

where f is the frequency with the unit Hz.

4. **Result and Analysis.** The model parameters of the suspension system are as follows: the masses of the spring-loaded part and the unsprung part are 340kg and 40kg, respectively; the damping coefficient of the damper is 1400Ns/m; the stiffness coefficients of the semi-active suspension and the tire are 17kN/m and 190kN/m, respectively. The controllable force in the semi-active suspension system is limited. If the control force is greater than the gravity of the unsprung mass, the probability of the wheel leaving the ground will increase. This will affect the grip performance of the wheel. The maximum controllable force is 350N in this study.

The numerical computation schematic diagram of the semi-active suspension control is shown in Figure 4 based on the Runge-Kutta method. The schematic diagram can be expressed as follows.

Step 1: The initial value of the control system is determined. The initial value includes the initial suspension displacement, bodywork displacement, suspension speed, bodywork speed and control force.

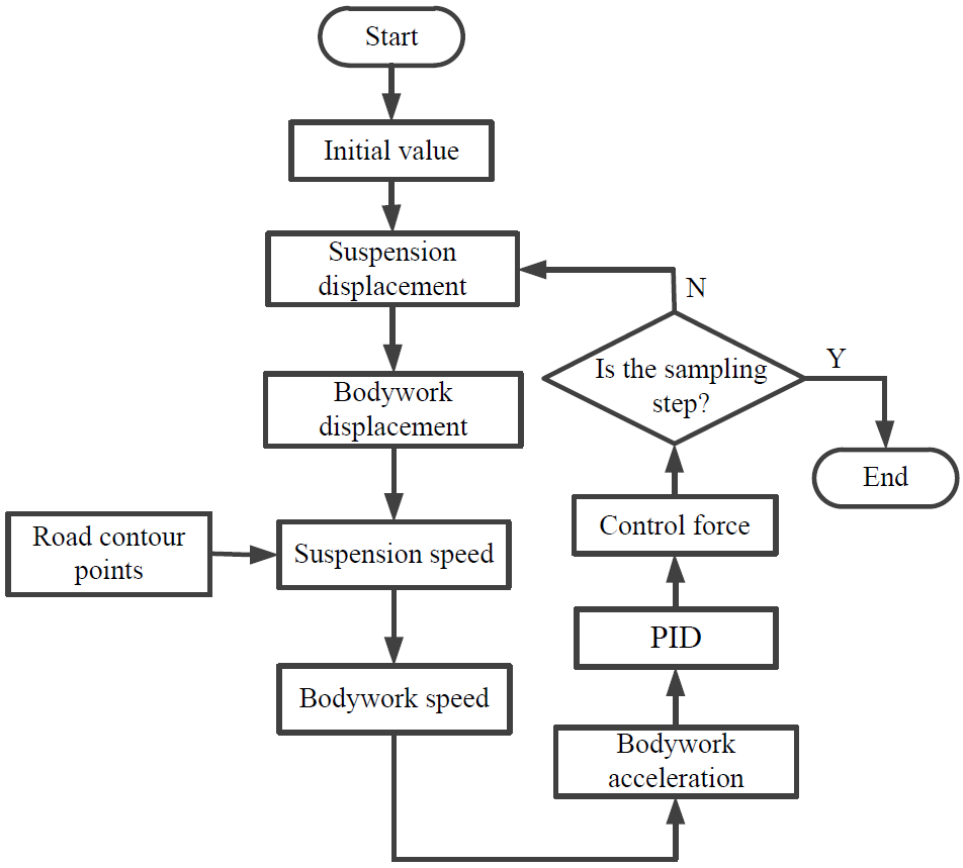

FIGURE 4. Numerical computation schematic diagram of the semi-active suspension control

Step 2: The instant suspension displacement is obtained using Equation (2a). The suspension displacement parameter is replaced by the instant suspension displacement.

Step 3: The instant bodywork displacement is obtained using Equation (2b). The bodywork displacement parameter is updated by the instant bodywork displacement.

Step 4: The suspension displacement, bodywork displacement, road profile point, suspension speed, bodywork speed, and control force are substituted into Equation (2c) to determine the instant suspension speed. The suspension displacement and the bodywork displacement values are obtained in Steps 2 and 3. The road profile point is obtained by the road surface excitation model. The suspension speed value is updated.

Step 5: The suspension displacement, bodywork displacement, suspension speed, bodywork speed, and control force are substituted into Equation (2d) to determine the bodywork speed at this moment. The suspension displacement, bodywork displacement and suspension speed parameters are obtained in Steps 2 to 4. The bodywork speed parameter is replaced by the bodywork speed at the moment.

Step 6: The suspension displacement, bodywork displacement, suspension speed, bodywork speed, and control force are substituted into Equation (2d) to determine the bodywork acceleration at this moment. The suspension displacement, bodywork displacement, suspension speed and bodywork speed parameters are obtained in Steps 2 to 5. The bodywork acceleration value is updated by the bodywork acceleration value at this moment.

Step 7: The control force is computed using the PID controller through the bodywork acceleration error as the PID controller input. The performance of the semi-active suspension is changed to adjust the control force through the PID controller.

Step 8: The time variable t is updated by an increment. If the stop condition is reached, the computation is completed; else, go to Step 2.

The road profile is obtained by Equation (12) for that the vehicle runs at different speeds and on different road surfaces. The road profile is determined by two key parameters: the vehicle speed and the white noise. The 5 C-level road profiles are shown in Figure 5 with the following key parameters.

(1) Road 1: the vehicle speed is 10m/s, and the white noise is 1.
(2) Road 2: the vehicle speed is 28m/s, and the white noise is 1.
(3) Road 3: the vehicle speed is 20m/s, and the white noise is 2.
(4) Road 4: the vehicle speed is 20m/s, and the white noise is 3.
(5) Road 5: the vehicle speed is 20m/s, and the white noise is 4.

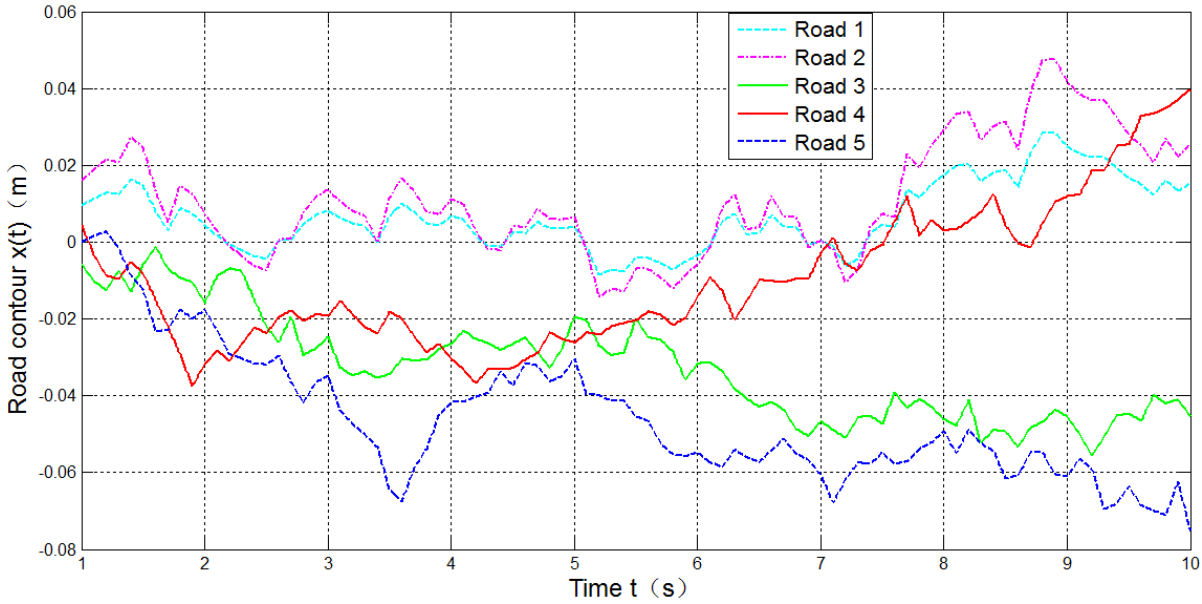

FIGURE 5. Road profile in the time domain

As can be seen from Road 1 and Road 2 in Figure 5, the road profile curve shape has the same shape under the same white noise parameter, and the amplitude of the road surface profile is determined by the vehicle speed v. From Equation (12), the amplitude is proportional to $\sqrt{v}$. As a whole, the amplitude is proportional to the white noise parameter from Road 3, Road 4 and Road 5, which can also be explained using Equation (12).

In what follows, the comprehensive computation and comparison of the semi-active suspension are verified and demonstrated using three PID controllers, namely the classical PID controller, the integral separation PID controller and the incomplete differential PID controller. The optimal control parameters are obtained by using the genetic algorithm. The optimal PID controller parameters are shown in Table 1 for a C-level road profile (called Road 6) with the key parameters the vehicle speed 20m/s and the white noise 1.

TABLE 1. Optimal PID controller parameters

	k_{p}	k_{i}	k_{d}	Integral threshold
Classical PID	−930.079	−19490.016	3.704	–
Integral separation PID	−956.450	−16172.154	3.773	274.777
Incomplete differential PID	−327.624	−18638.124	−43.735	–

4.1. **Test on a C-level road.** As shown in Figure 6, when the vehicle runs on Road 6, the vertical bodywork acceleration with the passive suspension is about $-0.82 \sim 0.9\text{m/s}^2$. The vertical bodywork acceleration is approximately between -0.4 and 0.42m/s^2 if the semi-active suspension is controlled by the classical PID controller, the integral separation PID controller and the incomplete derivative PID controller. The bodywork acceleration amplitude with the semi-active suspension controlled by the PID controller is significantly reduced compared with the passive suspension.

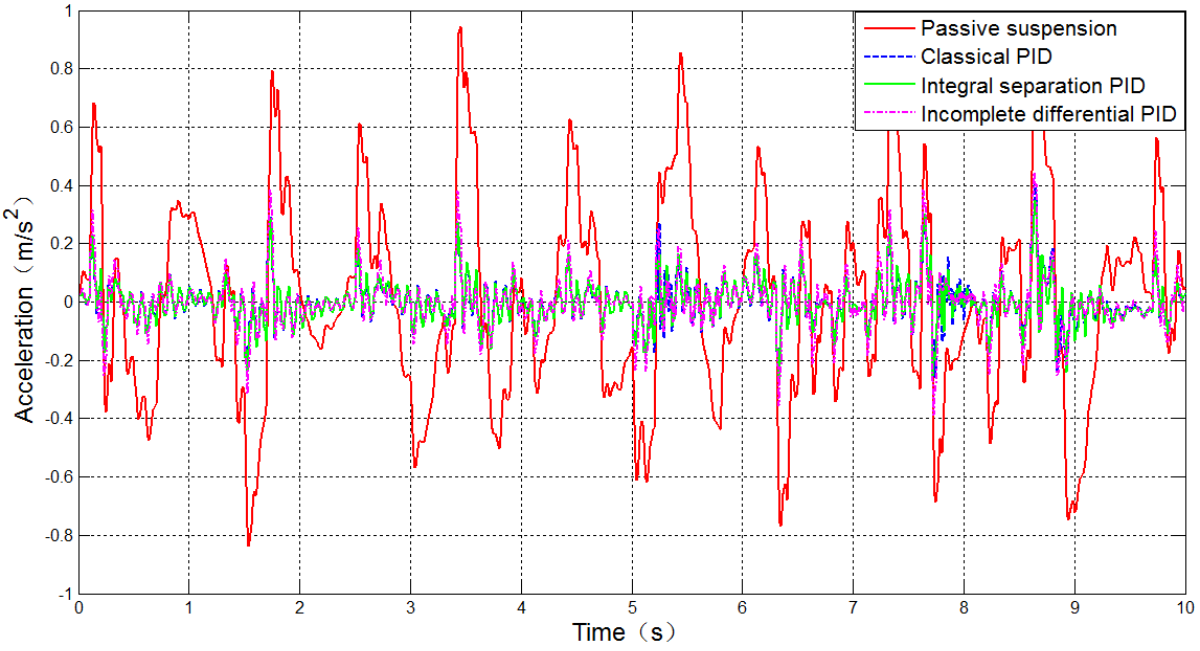

FIGURE 6. Vertical acceleration of the bodywork

As shown in Figure 7, the bodywork speed with the passive suspension is between -0.12 and 0.1m/s in the vertical direction. The bodywork speed with the semi-active suspension controlled by the PID controller is only approximately between -0.02 and 0.03m/s in the vertical direction. Compared with the passive suspension, the speed amplitude is evidently reduced with the semi-active suspension controlled by the PID controller. The bodywork speed change rate with the passive suspension is the largest in Figure 7. Therefore, the performance of the semi-active suspension controlled by the PID controller is excellent.

As shown in Figure 8, the bodywork displacement with the passive suspension is between about -0.02m and 0.045m in the vertical direction. When the semi-active suspension is controlled by the PID controller, the vertical bodywork displacement is approximately between -0.002m and -0.03m. The vertical bodywork displacement amplitude is significantly smaller than that of the passive suspension. The bodywork vertical displacement change rate of the passive suspension is the largest.

As shown in Figure 9, the suspension deflection of the passive suspension is approximately between -0.012 and 0.013m. The suspension deflections are approximately between -0.018 and 0.024m for the classical PID controller, the integral separation PID controller and the incomplete differential PID controller. Therefore, the deflection range of the semi-active suspension is larger than the passive suspension.

The performance comparison between the passive and the semi-active suspensions is shown in Table 2. The weighted acceleration RMS value of the bodywork with the passive suspension is 0.2888m/s^2 in the vertical direction. The bodywork displacement RMS value of the passive suspension is 0.0164m in the vertical direction. The vertical bodywork

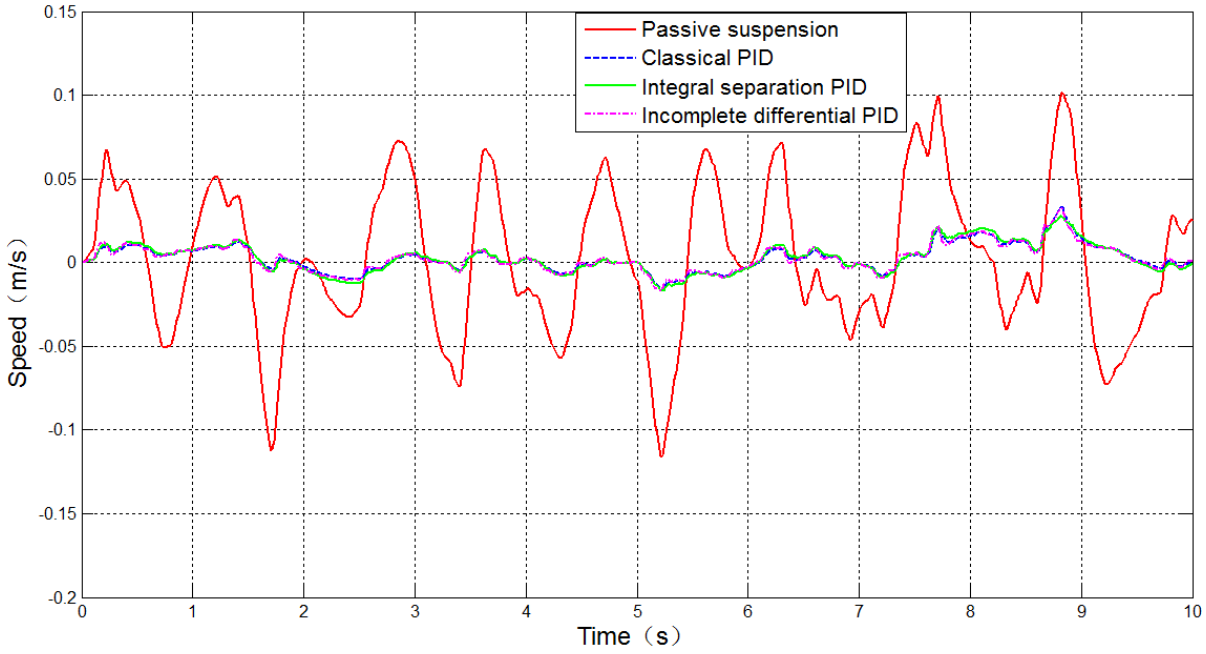

FIGURE 7. Vertical speed of the bodywork

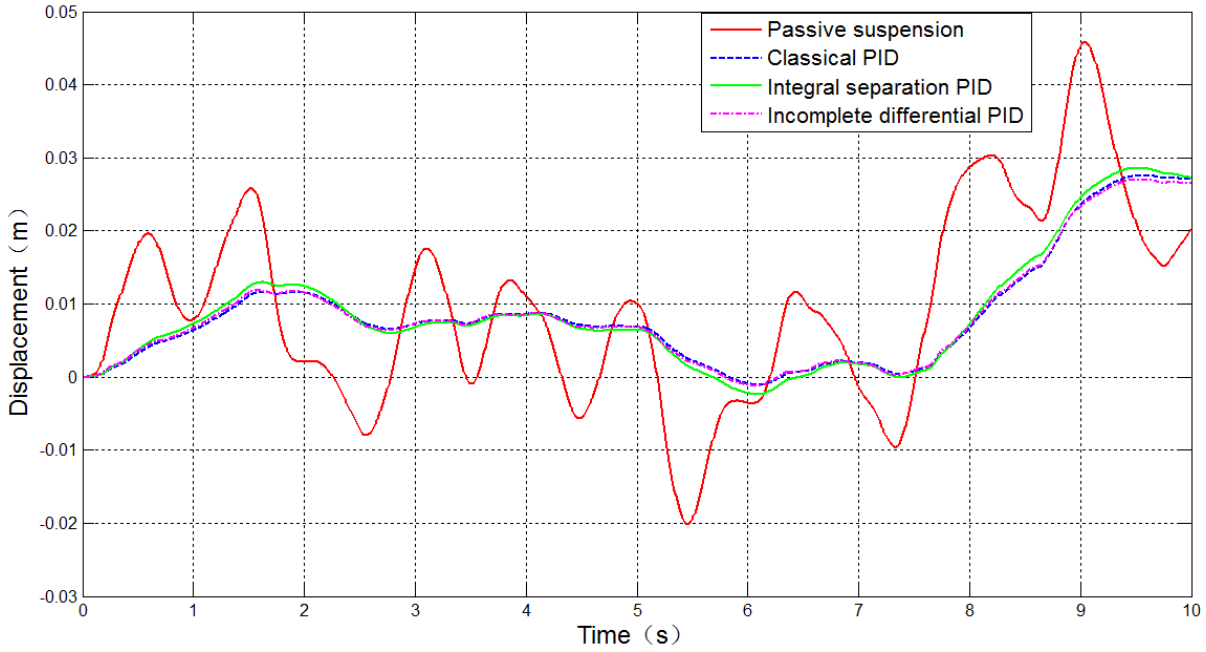

FIGURE 8. Vertical displacement of the bodywork

speed RMS value of the passive suspension is 0.0450m/s. If the suspension is controlled by the classical PID controller, the weighted acceleration RMS value of the bodywork is 0.0286m/s^2 in the vertical direction. The weighted acceleration RMS value of the bodywork is reduced by 90.1% compared with the passive suspension. The vertical bodywork speed RMS value of the suspension is 0.0084m/s. The bodywork speed RMS value is reduced by 81.3% compared with the passive suspension. The vertical bodywork displacement RMS value of the suspension is 0.0113m. The bodywork displacement RMS value is reduced by 31.1% compared with the passive suspension. The RMS value of the control force is 166.0545N.

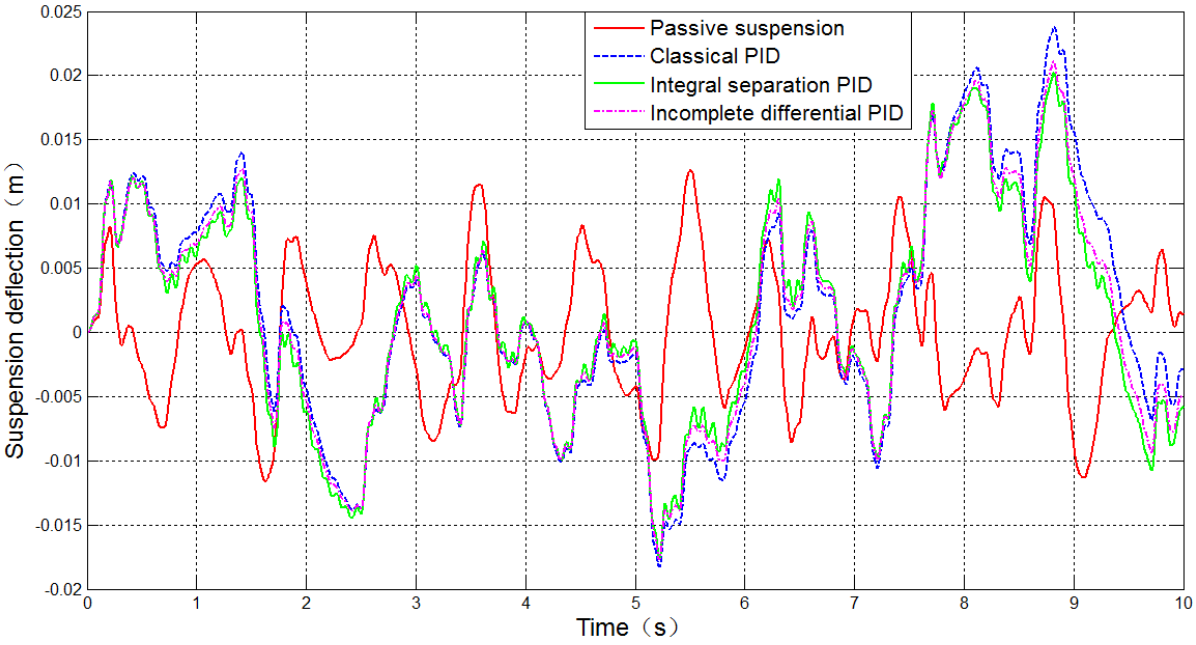

FIGURE 9. Vertical deflection of the suspension

TABLE 2. Performance comparison between the passive and semi-active suspensions on a C-level road

	Passive suspension	Classical PID		Integral separation PID		Incomplete differential PID	
	RMS value	RMS value	Decrease rate	RMS value	Decrease rate	RMS value	Decrease rate
Weighted acceleration (m/s^2)	0.2888	0.0286	90.1%	0.0316	89.1%	0.0332	88.5%
Displacement (m)	0.0164	0.0113	31.1%	0.0118	28.0%	0.0112	31.7%
Speed (m/s)	0.0450	0.0084	81.3%	0.0091	79.8%	0.0085	81.1%
Control force (N)	–	166.0545	–	159.9322	–	158.8368	–

When the semi-active suspension is controlled by the integral separation PID controller, the weighted acceleration RMS value of the bodywork is 0.0316m/s^2 in the vertical direction. Compared with the passive suspension, the weighted acceleration RMS value of the bodywork is reduced by 89.1% in the vertical direction. The RMS value of the bodywork speed is 0.0091m/s in the vertical direction. The RMS value of the bodywork speed is reduced by 79.8% in the vertical direction compared with the passive suspension. The bodywork displacement RMS value of the suspension is 0.0118m in the vertical direction. The RMS value of the bodywork displacement is reduced by 28.0% compared with the passive suspension. The RMS value of the control force is 159.9322N.

The weighted bodywork acceleration RMS value of the semi-active suspension controlled by the incomplete differential PID controller is 0.0332m/s^2 in the vertical direction. When the suspension is controlled by the incomplete differential PID controller, the weighted acceleration RMS value of the bodywork is reduced by 88.5% compared with the passive

suspension. The RMS value of the bodywork speed of the suspension is 0.0085m/s in the vertical direction. The RMS value of the bodywork speed is reduced by 81.1% compare with the passive suspension. The bodywork displacement RMS value of the suspension is 0.0112m in the vertical direction. The RMS value of the bodywork displacement is reduced by 31.7% compared with passive suspension. The RMS value of the control force is 158.8368N.

The performance of the semi-active suspension controlled by the PID controller is superior to the passive suspension on the aspect of the weighted acceleration, the displacement and the bodywork speed. However, obvious performance difference can be found between different semi-active PID controllers. The weighted acceleration RMS value of the bodywork is smallest controlled by the classical PID controller. The bodywork weighted acceleration RMS value with the suspension controlled by the incomplete differential PID controller is the largest. The bodywork displacement RMS value is the smallest with the suspension controlled by the incomplete differential PID controller. The bodywork displacement RMS value is the largest with the suspension controlled by the integral separation PID controller. The bodywork speed RMS value is the smallest controlled by the classical PID controller. The bodywork speed RMS value with the suspension controlled by the integral separation PID controller is the largest. From Table 2, it can also be found that the suspension performance under the classical PID controller is the best among the four different suspensions on Road 6.

4.2. **Test under different vehicle speeds.** In what follows, the performances of the semi-active suspensions controlled by the three PID controllers are analyzed for that the vehicle runs at different speeds. The RMS value of the weighted acceleration, the displacement and the speed of the bodywork in the vertical direction are computed and shown in Table 3 for different vehicle speeds.

As can be seen in Table 3, the weighted vertical acceleration RMS value of the bodywork increases with the vehicle speed increasing if the vehicle runs under the same road

Table 3. Performance comparison between the passive and semi-active suspensions under different vehicle speeds

	Passive suspension	Classical PID		Integral separation PID		Incomplete differential PID	
Vehicle speed (m/s)	Weighted RMS value of bodywork (m/s^2)	Weighted RMS value of bodywork (m/s^2)	Decrease rate (%)	Weighted RMS value of bodywork (m/s^2)	Decrease rate (%)	Weighted RMS value of bodywork (m/s^2)	Decrease rate (%)
10	0.2042	0.0192	90.5975	0.0218	89.3242	0.0230	88.7365
12	0.2237	0.0211	90.5677	0.0239	89.3160	0.0251	88.7796
14	0.2416	0.0228	90.5629	0.0258	89.3212	0.0272	88.7417
16	0.2583	0.0245	90.5149	0.0277	89.2760	0.0291	88.7340
18	0.2739	0.0264	90.3614	0.0295	89.2296	0.0310	88.6820
20	0.2888	0.0286	90.0970	0.0316	89.0582	0.0332	88.5042
22	0.3028	0.0310	89.7622	0.0339	88.8045	0.0360	88.1110
24	0.3163	0.0341	89.2191	0.0364	88.4919	0.0389	87.7015
26	0.3292	0.0375	88.6087	0.0393	88.0620	0.0419	87.2722
28	0.3417	0.0408	88.0597	0.0424	87.5915	0.0450	86.8306

conditions. When the vehicle speed increases from 10m/s to 28m/s, the weighted acceleration RMS value of the bodywork with the passive suspension increases from 0.2042m/s^2 to 0.3417m/s^2. When the vehicle speed increases from 10m/s to 28m/s, the weighted acceleration RMS value of the bodywork increases from 0.0192m/s^2 to 0.0408m/s^2 for the semi-active suspension controlled by the classical PID controller. When the vehicle speed increases from 10m/s to 28m/s, the weighted acceleration RMS value of the bodywork increases from 0.0218m/s^2 to 0.0424m/s^2 for the semi-active suspension controlled by the integral separation PID controller. When the vehicle speed increases from 10m/s to 28m/s, the weighted acceleration RMS value of the bodywork increases from 0.0230m/s^2 to 0.0450m/s^2 for the semi-active suspension controlled by the incomplete differential PID controller. In the whole, the comfort of the vehicle is worse when the vehicle speed is greater.

When the vehicle speed increases from 10m/s to 28m/s, the bodywork weighted acceleration RMS value percentage is reduced from 90.5975% to 88.0597% for the semi-active suspension controlled by the classical PID controller. When the vehicle speed increases from 10m/s to 28m/s, the bodywork weighted acceleration RMS value decrease percentage is reduced from 89.3242% to 87.5915% for the semi-active suspension controlled by the integral separation PID controller. When the vehicle speed increases from 10m/s to 28m/s, the bodywork weighted acceleration RMS value is reduced from 88.7365% to 86.8306% for the semi-active suspension controlled by the incomplete derivative PID controller.

As shown in Figure 10, when the vehicle speed is between 10m/s and 16m/s, the decrease rate of the bodywork acceleration is very small using the three PID controllers. When the vehicle speed increases from 16m/s to 28m/s, the decrease rate of the bodywork weighted acceleration RMS value is reduced. The decrease rate decreases with the increase of the vehicle speed. The computation results show that the weighted acceleration RMS value of the bodywork is always the smallest in the vertical direction when the semi-active suspension is controlled by the classical PID controller. When the suspension is controlled by the incomplete differential PID controller, the weighted acceleration RMS value of the

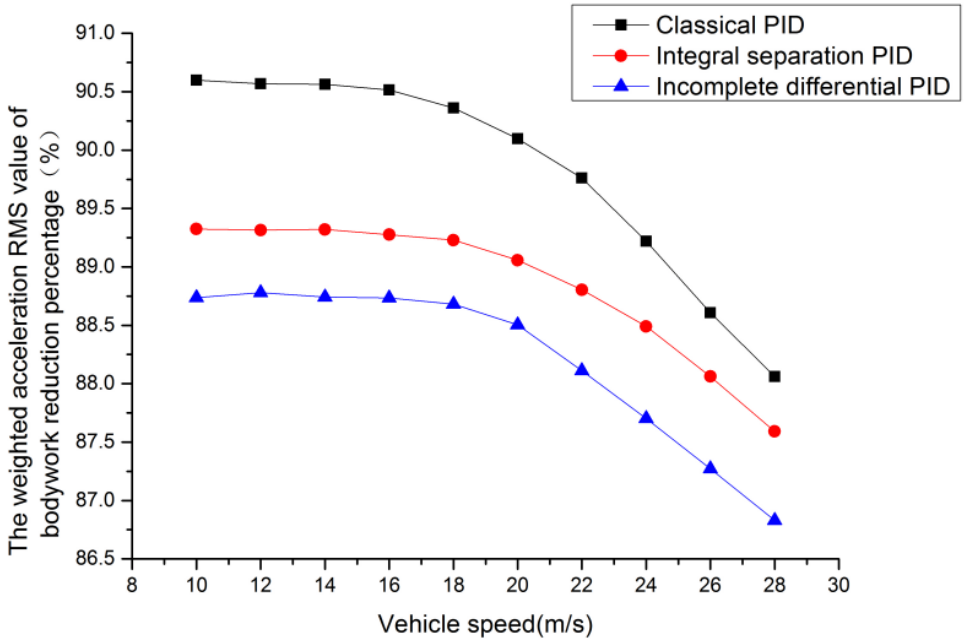

FIGURE 10. Weighted acceleration RMS value of the bodywork under different vehicle speeds

bodywork is always the largest in the vertical direction. In summary, the classical PID controller suspension has the best performance.

As shown in Figure 11, the displacement RMS value of the bodywork increases with the increase of the vehicle speed in the vertical direction. The displacement RMS value of the bodywork of the suspension controlled by the integral separation PID controller is always the largest in the vertical direction. There is no obvious difference between the classical PID controller and the incomplete differential PID controller. To sum up, when the vehicle runs at different speeds, the vehicle ride comfort is the best controlled by the classical PID controller.

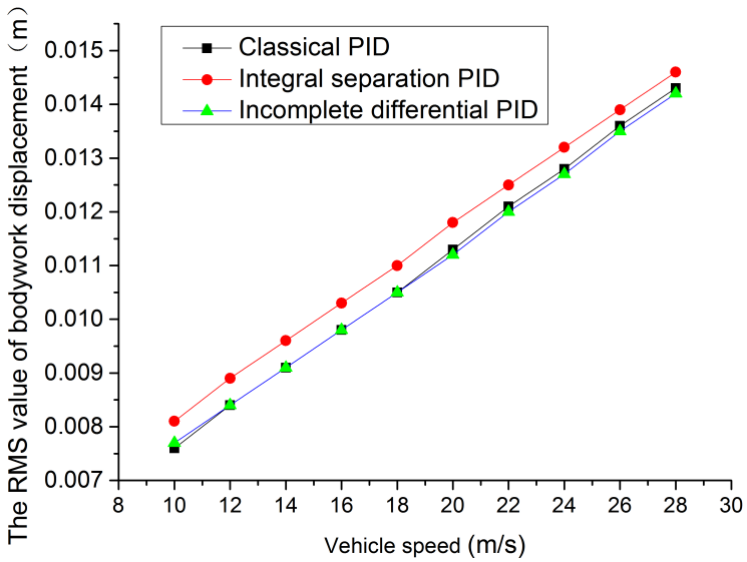

FIGURE 11. Bodywork vertical displacement RMS value under different vehicle speeds

4.3. **Test at different roads.** In order to comprehensively compare the adaptability of the suspension using different PID controller, the optimal parameter based on Road 6 is used. When the vehicle runs on Road 3, the acceleration and speed of the bodywork are shown in Figures 12 and 13. As shown in Figure 12, when the suspension is separately controlled by the classical PID controller and the integral separation PID controller, there is no obvious difference in the change rate of the bodywork acceleration at Road 3. When the vehicle runs on Road 3 and the suspension is controlled by the incomplete differential PID controller, both the bodywork acceleration and its change rate are the largest. The performance of the incomplete differential PID controller suspension is the worst compared with the other two PID controllers. As shown in Figure 13, when the vehicle runs on Road 3, the bodywork speed is the largest controlled by the incomplete differentiated PID controller suspension. The dynamic performance of the incomplete differential PID controller suspension is better than the other two PID controllers.

The performance of the semi-active suspension controlled by the three PID controllers is shown in Table 4. The result shows that the performance of the semi-active suspension using the PID controller is significantly improved compared with the passive suspension. With the control of the three PID controllers, the weighted acceleration RMS values of the bodywork are respectively 87.7%, 86.5% and 84.6% less than the passive suspension in the vertical direction. And the corresponding bodywork speed RMS values are respectively 74.7%, 73.4% and 74.1% less than the passive suspension in the vertical direction. When the suspension is controlled by the classical PID controller, the decrease rate of

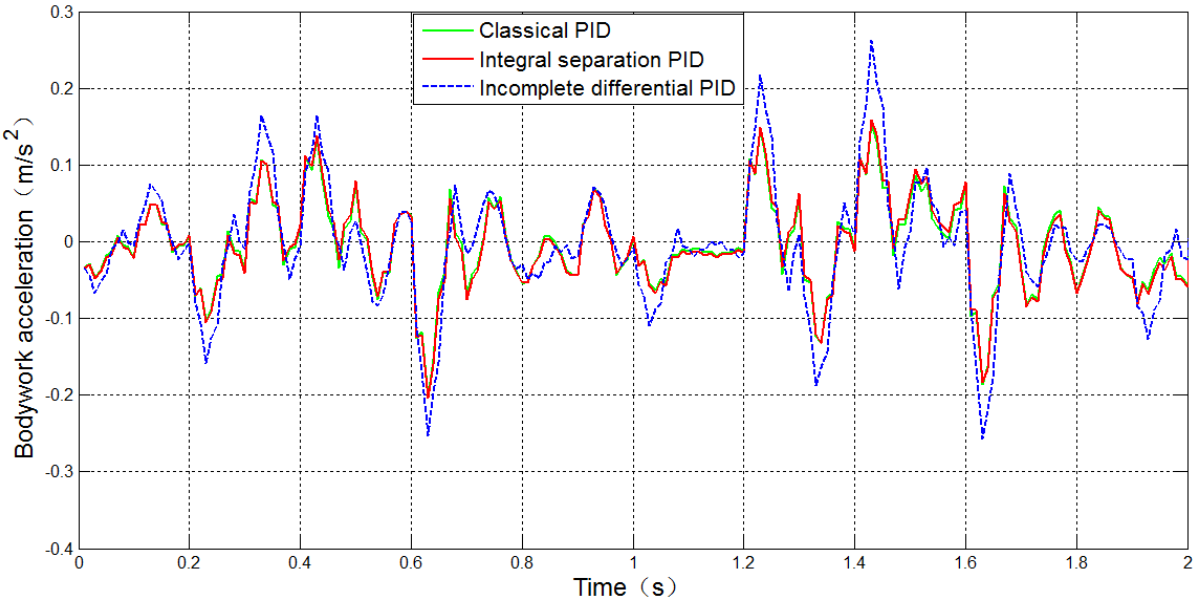

FIGURE 12. Bodywork vertical acceleration on Road 3 for the semi-active suspension controlled by the PID controller

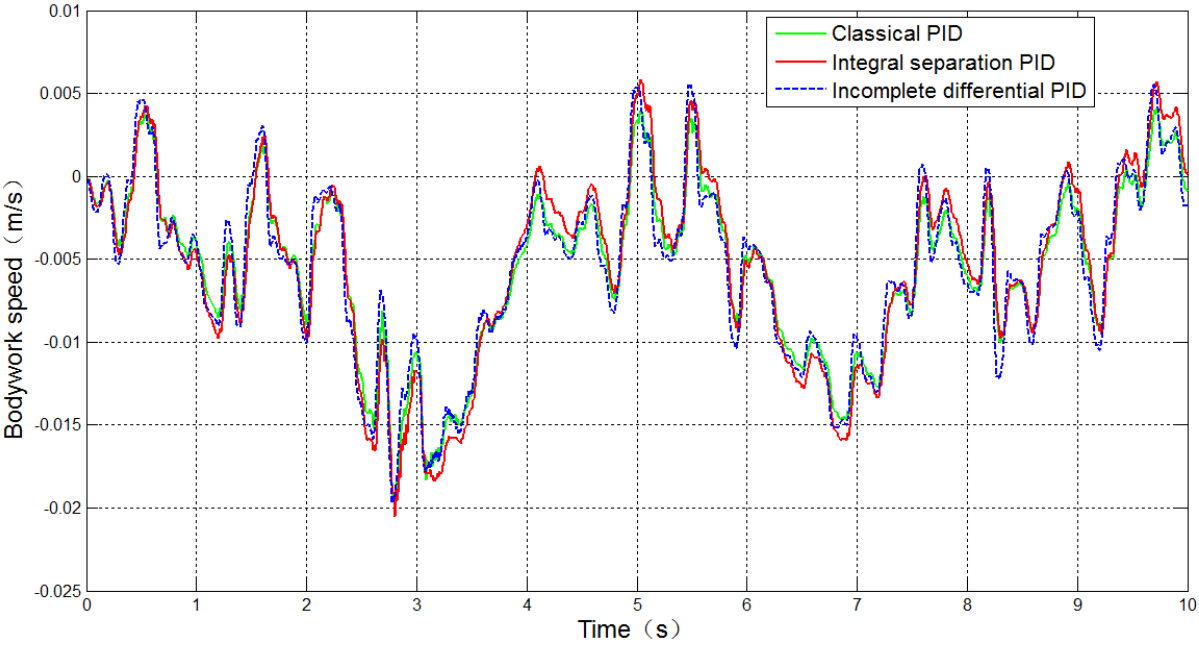

FIGURE 13. Bodywork vertical speed on Road 3 for the semi-active suspension controlled by the PID controller

the bodywork weighted acceleration RMS value and the speed RMS value is the largest in the vertical direction. When the vehicle runs on Road 3, the suspension performance using the classical PID controller is the best. The bodywork weighted acceleration RMS values of the semi-active suspension using the three PID controllers are respectively 80.1%, 81.4% and 79.2% less than the passive suspension in the vertical direction. And the bodywork speed RMS values are respectively 61.1%, 61.7% and 61.9% less than the passive suspension in the vertical direction.

The bodywork weighted acceleration RMS value of the semi-active suspension using the three PID controllers are respectively 74.7%, 77.9% and 74.0% less than the passive

TABLE 4. Performance of semi-active suspension on different roads

		Road 3	Road 4	Road 5	Road 7
Passive suspension	Weighted acceleration RMS value (m/s^2)	0.1712	0.1647	0.2559	0.2702
	Speed RMS value (m/s)	0.0293	0.0339	0.0402	0.0425
Classical PID	Weighted acceleration RMS value (m/s^2)	0.0211	0.0328	0.0647	0.0279
	Decrease (%)	87.7	80.1	74.7	89.7
	Speed RMS value (m/s)	0.0074	0.0132	0.0136	0.0094
	Decrease (%)	74.7	61.1	66.2	77.9
Integral separation PID	Weighted acceleration RMS value (m/s^2)	0.0231	0.0306	0.0565	0.0306
	Decrease (%)	86.5	81.4	77.9	88.7
	Speed RMS value (m/s)	0.0078	0.0130	0.0133	0.0097
	Decrease (%)	73.4	61.7	66.9	77.2
Incomplete differential PID	Weighted acceleration RMS value (m/s^2)	0.0264	0.0342	0.0666	0.0321
	Decrease (%)	84.6	79.2	74.0	88.1
	Speed RMS value (m/s)	0.0076	0.0129	0.0134	0.0094
	Decrease (%)	74.1	61.9	66.7	77.9

suspension in the vertical direction on Road 5. And the bodywork speed RMS values are respectively 66.2%, 66.9% and 66.7% less than the passive suspension in the vertical direction. When the suspension is controlled by the integral separation PID controller, the decrease rate of the weighted acceleration RMS value and the bodywork speed RMS value is the largest in the vertical direction. When the vehicle runs on Road 4 and Road 5, the suspension performance is the best for the integral separation PID controller.

When the road profile level is C, the vehicle speed is 20m/s, and the white noise is 5, a road profile is obtained and called Road 7 here. The bodywork weighted acceleration RMS values of the semi-active suspension using the three PID controllers are respectively 89.7%, 88.7% and 88.1% less than the passive suspension in the vertical direction on Road 7. And the bodywork speed RMS value is respectively 77.9%, 77.2% and 77.9% less than the passive suspension in the vertical direction. Therefore, it can be concluded that the suspension performance is greatly improved when the suspension is controlled by the three PID controllers on Road 7.

When the vehicle runs on different roads, the semi-active suspension controlled by the three PID controllers exhibits excellent performance compared with the passive suspension. There are always obvious differences between the three different PID controllers. From a whole point of view, the semi-active suspension controlled by the classical PID controller and the integral separation PID controller has better performance than the incomplete differential PID controller. The bodywork acceleration change controlled by the integral separation PID controller is smallest in the percent improvement. The performance of the integral separation PID controller is best in the three PID controllers.

It can be seen from the test on a C-level road that the bodywork acceleration, speed and displacement of the semi-active suspension controlled by the three PID controllers are significantly reduced compared with the passive suspension. However, the suspension deflection of the three semi-active suspensions becomes larger. This indicates that the ride

comfort performance of the semi-active suspension vehicle controlled by the three controllers is improved, while the wheel grip performance of the semi-active suspension vehicle is deteriorated. If the vehicle runs under the same road condition, the weighted vertical acceleration RMS value of the bodywork increases with the vehicle speed increasing and the semi-active suspension controlled by three PID controllers has strong adaptability at different vehicle speeds. Compared with the passive suspension, the bodywork weighted acceleration value of the suspension controlled by the classical PID controller is minimal in the three control suspensions. Therefore, the ride comfort of the suspension controlled by the classical PID controller is the best. When the vehicle runs on different roads, the performance of the semi-active suspension controlled by the three PID controllers is significantly improved compared with the passive suspension. The semi-active suspensions controlled by the three PID controllers have different adaptability. The adaptive performance of the semi-active suspension controlled by the integral separation PID controller is best in the three PID controllers.

5. **Conclusions.** The suspension dynamics mathematical model and the numerical analysis model are established based on the principle of the suspension dynamics. The suspension model is controlled by the classical PID controller, the integral separation PID controller and the incomplete differential PID controller respectively under different speeds and on the different road profile. The optimal control parameter is obtained using the genetic algorithm. The performance characteristics of the vehicle semi-active suspension are studied under different controllers and road conditions. The analysis results show that the performance of the semi-active suspension controlled by the three PID controllers is greatly improved compared with the passive suspension.

The performance of semi-active suspension controlled by the three PID controllers is analyzed when the vehicle runs on the same road under the different speeds. The weighted acceleration RMS value of the bodywork is always the smallest when the semi-active suspension is controlled by the classical PID controller. Therefore, when the vehicle runs at different speeds, the vehicle ride comfort is the best controlled by the classical PID controller. The performance of semi-active suspension controlled by the three PID controllers is analyzed when the vehicle runs on different roads under the same speed. The three controllers for semi-active suspension have different adaptability on the different road conditions. The bodywork acceleration change controlled by the integral separation PID controller is smallest in the percent improvement. Therefore, when the vehicle runs on different roads at the same speed, the adaptive performance of the semi-active suspension controlled by the integral separation PID controller is best.

In terms of vehicle performance, roads have the greatest impact on suspension performance. All in all, the integral separation PID controller has the best performance. The study lays a foundation for the semi-active suspension experiments, the dynamic analysis and the optimization design of suspension structure.

Acknowledgments. This work is supported by National Natural Science Foundation of China (No. U1304525) and Henan Polytechnic University Doctoral Science Foundation (No. B2013-027, 648495). The authors would like to thank the anonymous reviewers for their valuable work.

REFERENCES

[1] L. C. Felix-Herran, J. J. Rodriguez-Ortiz and R. Soto, Semi-active vehicle suspension fuzzy control with a magnetorheological damper including the actuator dynamics, *Proc. of the Mini Conference on Vehicle System Dynamics, Identification and Anomalies*, Budapest, pp.613-620, 2008.

[2] L. Khan, M. U. Khan and S. Qamar, Comparative analysis of suspension systems using adaptive fuzzy control, *The 4th International Conference on Intelligent and Advanced Systems: A Conference of World Engineering, Science and Technology Congress (ESTCON)*, Kuala Lumpur, pp.22-27, 2012.
[3] M. A. Talib and I. M. Darus, Self-tuning PID controller with MR damper and hydraulic actuator for suspension system, *The 5th International Conference on Computational Intelligence*, Seoul, pp.119-124, 2013.
[4] A. Giua, M. Melas, C. Seatzu and G. Usai, Design of a predictive semi-active suspension system, *Vehicle System Dynamics*, vol.41, pp.277-300, 2014.
[5] F. Kou, J. Du, Z. Wang, D. Li and J. Xu, Nonlinear modeling and coordinate optimization of a semi-active energy regenerative suspension with an electro-hydraulic actuator, *Algorithms*, vol.11, no.12, pp.1-17, 2018.
[6] A. Pascoal, J. Goncalves and M. Braz-Cesar, Dynamic analysis and comfort evaluation of a full suspension bicycle equipped with a MR damper, *Proc. of the 6th International Conference on Computational Methods in Structural Dynamics and Earthquake Engineering*, Rhodes Island, pp.3128-3133, 2017.
[7] W. Yang, *Research on Design and Experiment of Multi-level Adjustable Damping Semi-active Suspension Control Based on Multi-operating Conditions for a Sedan*, Master Thesis, Jilin University, 2017.
[8] O. Demir, I. Keskin and S. Cetin, Modeling and control of a nonlinear half-vehicle suspension system: A hybrid fuzzy logic approach, *Nonlinear Dynamics*, vol.67, no.3, pp.2139-2151, 2012.
[9] C. T. Wang, H. T. Liu, F. W. Xie, J. Zhang and E. M. Ding, Analysis of dynamic characteristics of semi-active suspension based on expert system, *Automation & Instrumentation*, vol.3, no.3, pp.1-4+13, 2018.
[10] S. Sulaiman, P. M. Samin and H. Jamaluddin, Dynamic tire force control for light-heavy duty truck using semi active suspension system, *The 2nd International Conference on Computer, Communications and Control Technology*, Kuching, pp.98-102, 2015.
[11] K. Rajeswari and P. Lakshmi, Simulation of suspension system with intelligent active force control, *Proc. of the 2nd International Conference on Advances in Recent Technologies in Communication and Computing*, Jakarta Barat, pp.271-277, 2010.
[12] A. B. Kunya and A. A. Ata, Half car suspension system integrated with PID controller, *Proc. of the 29th European Conference on Modelling and Simulation*, Varna, pp.233-238, 2015.
[13] J. X. Tang, T. Zhang and S. S. Niu, The semi-active air spring for PID optimal control and co-simulation, *Automobile Applied Technology*, vol.1, pp.55-58, 2018.
[14] N. H. Amer, R. Ramli and W. L. Wan Mahadi, Implementations of PID controller and its transient behavior in active suspension system, *Advanced Materials Research*, vol.895, pp.490-499, 2014.
[15] D. Hanafi, PID controller design for semi-active car suspension based on model from intelligent system identification, *The 2nd International Conference on Computer Engineering and Applications*, Indonesia, pp.60-63, 2010.
[16] N. L. V. Truong, V. D. Do, V. T. Nguyen and T. H. Phan, Analytical design of PID controller for enhancing ride comfort of active vehicle suspension system, *Proc. of International Conference on System Science and Engineering*, Ho Chi Minh City, pp.305-308, 2017.
[17] P. Anantachaisilp and Z. Lin, Fractional order PID control of rotor suspension by active magnetic bearings, *Actuators*, vol.6, no.4, pp.1-31, 2017.
[18] N. Desai and B. Kale, Performance evaluation of quarter car model semi active suspension system with fuzzy logic system, *International Conference on Advances in Computing, Communication and Control (ICAC3)*, Mumbai, India, pp.1-5, 2017.
[19] A. Alfadhli, J. Darling and A. J. Hillis, The control of an active seat suspension using an optimized fuzzy logic controller based on preview information from a full vehicle model, *Vibration*, vol.1, pp.20-40, 2018.
[20] X. M. Ye, H. Y. Long, W. C. Pei, Y. G. Li and S. Zheng, Fuzzy control for automotive semi-active suspension with MR damper, *Journal of North China University of Science and Technology (Natural Science Edition)*, vol.40, no.2, pp.96-99, 2018.
[21] R. Rakhsha, S. A. Ghazavi and N. Yasrebi, Using fuzzy logic to control active suspension system of one-quarter-car model, *The 13th International Congress on Sound and Vibration*, Vienna, pp.3440-3448, 2006.
[22] P. Senthilkumar, K. Sivakumar, R. Kanagarajan and S. Kuberan, Fuzzy control of active suspension system using full car model, *Mechanika*, vol.24, no.2, pp.240-247, 2018.

[23] M. Zeinali, S. A. Mazlan and M. A. A. Rahmanc, Influence of fuzzy-PID controller on semi-active suspension system performance using magnetorheological damper fuzzy model, *Applied Mechanics and Materials*, vol.663, pp.243-247, 2014.
[24] K. Cao, W. W. Wang, L, Q. Chen and W. W. Dong, Fuzzy parameter self-tuning PID control of electronically controlled air suspension system, *Journal of Shandong Jiaotong University*, vol.25, pp.1-8, 2017.
[25] R. Kashani and S. Kiriczi, Robust stability analysis of LQG-controlled active suspension with model uncertainty using structured singular value method, *Vehicle System Dynamics*, vol.21, no.6, pp.361-384, 1992.
[26] Y. Jin, D. J. Yu, Z. X. Chen, M. H. Jiang and X. He, Endocrine LQR control strategy and its application in vibration suppression by active suspensions, *Journal of Vibration and Shock*, vol.35, no.10, pp.49-54, 2016.
[27] J. Luczko and U. Ferdek, Continuous and discrete sliding mode control of an active car suspension system, *Journal of Theoretical and Applied Mechanics*, vol.54, no.1, pp.3-11, 2016.
[28] S. Toyama and F. A. Ikeda, Sliding mode control of semi-active suspension systems with describing function method, *Nihon Kikai Gakkai Ronbunshu, C Hen/Transactions of the Japan Society of Mechanical Engineers*, vol.79, pp.459-468, 2013.
[29] H. Li, Y. H. Feng and L. W. Su, Vehicle active suspension vibration control based on robust neural network, *Chinese Journal of Construction Machinery*, vol.15, no.4, pp.324-328+337, 2017.
[30] A. Suebsomran, Adaptive neural network control of electromagnetic suspension system, *International Journal of Robotics and Automation*, vol.29, no.2, pp.144-154, 2014.
[31] B. K. Song, J. H. An and S. B. Choi, A new fuzzy sliding mode controller with a disturbance estimator for robust vibration control of a semi-active vehicle suspension system, *Appl. Sci.*, vol.7, pp.1-20, 2017.
[32] H. Souilem and N. Derbel, Neuro-fuzzy control of vehicle active suspension system, *International Journal of Circuits, Systems and Signal Processing*, vol.12, pp.423-431, 2018.
[33] J. Meng, H. P. Yang, Q. Z. Chen and K. Zhang, Simulation research of the PID controller of vehicle suspension based on the genetic algorithm, *Modern Manufacturing Engineering*, vol.6, pp.92-96, 2013.
[34] W. Wang, Y. Song, Y. Xue, H. Jin, J. Hou and M. Zhao, An optimal vibration control strategy for a vehicle's active suspension based on improved cultural algorithm, *Applied Soft Computing*, vol.28, pp.167-174, 2015.
[35] H. Metered, A. Elsawaf and T. Vampola, Vibration control of MR-damped vehicle suspension system using PID controller tuned by particle swarm optimization, *SAE International Journal of Passenger CARS – Mechanical Systems*, vol.8, no.2, pp.426-435, 2015.
[36] K. Rajeswari and P. Lakshmi, PSO optimized fuzzy logic controller for active suspension system, *Proc. of the 2nd International Conference on Advances in Recent Technologies in Communication and Computing*, Jakarta Barat, pp.278-283, 2010.
[37] M. S. Sadeghi, S. Varzandian and A. Barzegar, Optimization of classical PID and fuzzy PID controllers of a nonlinear quarter car suspension system using PSO algorithm, *The 1st International Conference on Computer and Knowledge Engineering*, Mashhad, pp.172-176, 2011.
[38] P. Pannil, T. Sungsorn, T. Trisuwannawat and P. Ukakimaparn, Design of discrete-time PIDA controller using Kitti's method with first-order hold discretization, *ICIC Express Letters*, vol.12, no.6, pp.567-574, 2018.
[39] Z. S. Yu, *Automobile Theory*, China Machine Press, Beijing, 2016.